

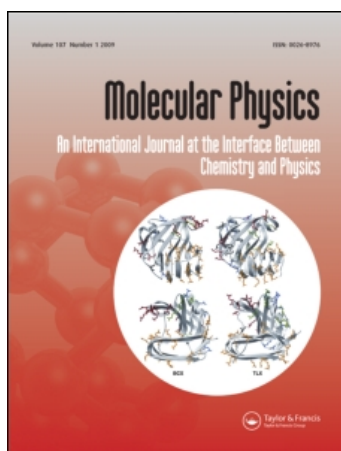
This article was downloaded by: [CAS Consortium]

On: 7 May 2009

Access details: Access Details: [subscription number 909168893]

Publisher Taylor & Francis

Informa Ltd Registered in England and Wales Registered Number: 1072954 Registered office: Mortimer House, 37-41 Mortimer Street, London W1T 3JH, UK



Molecular Physics

Publication details, including instructions for authors and subscription information:

<http://www.informaworld.com/smpp/title-content=t713395160>

Quantum Monte Carlo study of the CO interaction with a dimer model surface for Cr (110)

O. El Akramine ^a; W. A. Lester Jr ^a; X. Krokidis ^b; C. A. Taft ^c; T. C. Guimaraes ^d; A. C. Pavao ^d; R. Zhu ^e

^a Chemical Sciences Division, Lawrence Berkeley National Laboratory and Department of Chemistry, Kenneth S. Pitzer Center for Theoretical Chemistry, University of California, Berkeley, CA 94720-1460, USA.

^b Accelrys, Materials Science, 20 Rue Jean Rostand, F-91898 Orsay Cedex, France. ^c Centro Brasileiro de Pesquisas Fisicas, Rua Dr Xavier Sigaud 150, Rio de Janeiro RJ, Cep 22290-180 Brazil. ^d Departamento de Quimica Fundamental, Universidade Federal de Pernambuco, 50740-540 Recife, Pernambuco, Brazil. ^e LNM, Institute of Mechanics, Chinese Academy of Sciences, People's Republic of China.

Online Publication Date: 01 January 2003

To cite this Article Akramine, O. El, Lester Jr, W. A., Krokidis, X., Taft, C. A., Guimaraes, T. C., Pavao, A. C. and Zhu, R. (2003) 'Quantum Monte Carlo study of the CO interaction with a dimer model surface for Cr (110)', *Molecular Physics*, 101:1, 277 — 285

To link to this Article: DOI: 10.1080/00268970210162844

URL: <http://dx.doi.org/10.1080/00268970210162844>

PLEASE SCROLL DOWN FOR ARTICLE

Full terms and conditions of use: <http://www.informaworld.com/terms-and-conditions-of-access.pdf>

This article may be used for research, teaching and private study purposes. Any substantial or systematic reproduction, re-distribution, re-selling, loan or sub-licensing, systematic supply or distribution in any form to anyone is expressly forbidden.

The publisher does not give any warranty express or implied or make any representation that the contents will be complete or accurate or up to date. The accuracy of any instructions, formulae and drug doses should be independently verified with primary sources. The publisher shall not be liable for any loss, actions, claims, proceedings, demand or costs or damages whatsoever or howsoever caused arising directly or indirectly in connection with or arising out of the use of this material.

Quantum Monte Carlo study of the CO interaction with a dimer model surface for Cr(110)

O. EL AKRAMINE¹, W. A. LESTER JR^{1*}, X. KROKIDIS², C. A. TAFT³,
T. C. GUIMARAES⁴, A. C. PAVAO⁴ and R. ZHU⁵

¹ Chemical Sciences Division, Lawrence Berkeley National Laboratory and
Department of Chemistry, Kenneth S. Pitzer Center for Theoretical Chemistry,
University of California, Berkeley, CA 94720-1460, USA

² Accelrys, Materials Science, 20 Rue Jean Rostand, F-91898 Orsay Cedex, France

³ Centro Brasileiro de Pesquisas Fisicas, Rua Dr Xavier Sigaud 150, Rio de Janeiro
RJ, Cep 22290-180 Brazil

⁴ Departamento de Quimica Fundamental, Universidade Federal de Pernambuco,
50740-540 Recife, Pernambuco, Brazil

⁵ LNM, Institute of Mechanics, Chinese Academy of Sciences, People's Republic of
China

(Received 30 November 2001; accepted 6 May 2002)

The chemisorption of CO on a Cr(110) surface is investigated using the quantum Monte Carlo method in the diffusion Monte Carlo (DMC) variant and a model Cr₂CO cluster. The present results are consistent with the earlier *ab initio* HF study with this model that showed the tilted/near-parallel orientation as energetically favoured over the perpendicular arrangement. The DMC energy difference between the two orientations is larger (1.9 eV) than that computed in the previous study. The distribution and reorganization of electrons during CO adsorption on the model surface are analysed using the topological electron localization function method that yields electron populations, charge transfer and clear insight on the chemical bonding that occurs with CO adsorption and dissociation on the model surface.

1. Introduction

The interaction of diatomic molecules such as CO with transition metal (TM) surfaces is an important step in understanding heterogeneous catalysis. Evaluating quantitatively the interaction energy between a gas molecule and a TM surface, despite its importance, still presents computational difficulties; for recent reviews see [1, 2]. Much effort has been devoted to the investigation of the specific behaviour of each TM and the influence of the surface structure of the metal on the interaction with a diatomic molecule (see, e.g., [3]).

In a previous *ab initio* restricted Hartree–Fock (HF) study we considered Cr₂CO and Cr₄CO surface cluster models to simulate CO adsorption on the Cr(110) surface in perpendicular and tilted states [4]. The latter state was identified by us and others to account for the unusually low carbon–oxygen stretching observed in CO adsorption on TM surfaces and to be a predissociative molecular state [4].

In general, the direct and the precursor state models are used to describe the dissociation of a molecule on a surface [5]. In direct dissociative chemisorption the incident molecule dissociates into adsorbed fragments immediately upon collision with the surface. In dissociative chemisorption through a precursor state, the molecule is adsorbed intact before dissociating. It is well known that CO is adsorbed with the carbon atom closer to the surface. On most densely packed metal surfaces, CO is adsorbed with the molecular axis parallel to the surface normal [6]. We note that the more common Blyholder model [7] does not take into account the existence of CO tilted states [8] because at the time of publication there was no experimental evidence for their existence.

In this paper, we focus on CO adsorption and dissociation on a model transition metal surface for Cr(110). The Cr(110) surface is described by a Cr₂ system with the interatomic distance set to the experimental lattice separation of Cr(110). There have been numerous experimental investigations of CO chemisorption on single-crystal transition metals using various experimental techniques, including high resolution

* Author for correspondence. e-mail: WALester@lbl.gov

electron-energy-loss spectroscopy (HREELS), electron stimulated desorption ion angular distribution (ESDIAD), low energy electron diffraction (LEED), Auger electron spectroscopy (AES) [9], and core valence photoemission [10]. In addition, there have been a number of theoretical studies of the adsorption/dissociation of diatomic molecules on metallic surfaces, of which we cite only a few, using unrestricted Hartree–Fock (UHF) combined with resonating valence bond theory and multiple-scattering X_α formalism [6], The Hückel method [11], and *ab initio* UHF [12], in addition to the *ab initio* HF investigation of Cr_nCO clusters [4].

The aim of the present work is a quantum Monte Carlo (QMC) study in the diffusion Monte Carlo (DMC) approach of CO adsorption and dissociation on the Cr(110) model surface both to assess our previous *ab initio* HF study [4], and to gain insight into the use of the DMC method for quantitative description of gas–surface interactions. To these ends we compute the total energy of the system in the same configurations as previously investigated and identify the more stable binding mode. The DMC method has been successful in providing accurate descriptions of energies, including binding and atomization energies, ionization potentials, electron affinities [13–15], reaction barriers [16], and related properties. It had been used previously to study a number of TM systems [17–22].

The DMC method scales very favourably with system size, viz. N^3 , which is to be compared with other correlated methods that scale as N^6 or higher. The method is readily adaptable to parallel systems and has relatively modest memory requirements compared with the other high accuracy methods CI ($N!$) and coupled cluster (N^4) [23]. The usefulness of the DMC method has been demonstrated in many studies (for reviews, see, e.g., [24–26]). Due to the stochastic nature of the method, the computed DMC error depends on CPU time: longer simulations give more accurate results.

2. The quantum Monte Carlo method

The QMC method is a stochastic procedure for solving the time-dependent electronic Schrödinger equation in imaginary time. The imaginary-time evolution is accomplished using a density of ‘walkers’, each of which corresponds to a configuration of the system, i.e., corresponds to a set of particle positions. In the present study, as is common in molecular QMC applications, the nuclear positions are held fixed. The fixed-node DMC method leads to the following Schrödinger-like equation [24–26]:

$$\frac{\partial f}{\partial t} = \frac{1}{2} \nabla \cdot (\nabla - \mathbf{F}_q) f - (E_L - E_T) f. \quad (1)$$

We have introduced importance sampling to arrive at equation (1), which provides improved efficiency of the simulation. Here

$$f = \Psi_T \Phi, \quad (2)$$

where Ψ_T is a known approximate wavefunction, Φ is the exact solution and E_T is an energy offset. The quantity $\mathbf{F}_q = \ln |\Psi_T|^2$ is labelled the quantum force and has the effect of increasing sampling in the regions where the wavefunction is large (and thereby increases efficiency), and

$$E_L(\mathbf{R}) = \frac{\hat{H} \Psi_T(\mathbf{R})}{\Psi_T(\mathbf{R})}, \quad (3)$$

is the local energy, where \mathbf{R} denotes the $3N$ coordinates of the system. The evaluation of equation (3) for a broad range of randomly sampled coordinates or walkers from the distribution f using the Monte Carlo method leads to the DMC estimate of the energy.

The usual representation of a DMC trial wavefunction is in the form

$$\Psi_T = \psi \exp(U), \quad (4)$$

where typically ψ is an independent-particle-based function: Hartree–Fock, configuration interaction, or multi-configuration HF. The function U is chosen to be explicitly dependent on interparticle distance, i.e., $U(\{r_{ij}\}, \{r_{i\alpha}\}, \{r_{i\beta}\})$, where r_{ij} is the distance between electrons i and j , $r_{i\alpha}$ is the distance separating electron i and nuclear α and, $r_{i\beta}$ is the distance separating electron i and nucleus β . The two electron–nucleus terms describe density-dependent correlation. In the present study we have used the Schmidt–Moskowitz [27] function first introduced by Boys and Handy in the trans-correlated wavefunction method [28].

In this study we have used the short term approximation that characterizes the DMC method [24–26], and the Stevens–Basch–Krauss (SBK) effective core potentials (ECPs) [29]. The use of ECPs yields significant reduction in computer time because the detailed motion of the innermost electrons requires very small random-walk timesteps for high accuracy.

3. The electron localization function (ELF) method

The partitioning of molecular space into chemically significant regions remains an open challenge. In recent years topological theories of chemical bonding [30, 31, 33] have been formulated and applied [32, 34, 35] to analyse local quantum mechanical functions such as electronic density. One such function, Becke–Edgecombe’s electron localization function (ELF) [36], includes the capability of partitioning molecular space into basins corresponding to core and valence (attractor) regions, which helps one to understand the struc-

tural and chemical properties of a system, and to gain a deep insight into bond and lone pair localization. The picture of a molecule provided by the ELF analysis is consistent with Lewis valence theory, and enables one to assign chemical meaning to attractors and their basins. We have applied the topological ELF analysis to the Cr₂CO system.

The ELF function is defined by

$$\eta(\mathbf{r}) = \frac{1}{1 + \chi(\mathbf{r})}, \quad (5)$$

where $\chi(r)$ defines the ratio $D(r)/D_h(r)$. For a single determinant wavefunction, built from orbitals designated $\phi_i(r)$, the function $D(r)$ is given by

$$D(r) = \frac{1}{2} \sum_i |\nabla \phi_i(r)|^2 - \frac{1}{8} \frac{|\nabla \rho(r)|^2}{\rho(r)},$$

and expresses the excess of local kinetic energy due to Pauli repulsion [35]. The quantity $D_h(r) = C_F \rho(r)^{5/3}$ is the Thomas–Fermi kinetic energy density (uniform gas of electrons) [36], which here acts as a renormalization factor, and C_F is the Fermi constant ($C_F = 2.871$ au). The range of values of $\eta(r)$ is $0 \leq \eta \leq 1$. In a region of space with a single pair of electrons with anti-parallel spins, $\eta = 1$ due to the absence of Pauli repulsion between the electrons. In a region where two electrons with parallel spins come close the kinetic energy difference $D(r)$ becomes large (the two electrons avoid each other), and consequently $\eta \cong 0$. By construction for a uniform electron gas, $\eta = 0.5$. In principle, the ELF can be calculated from the exact wavefunction, if available, or from experimental results. In practice $\eta(r)$ is calculated from the natural orbitals, with no restriction on the quantum mechanical method used for obtaining them.

The partitioning of molecular space into regions where pairs of electrons (bonds, lone pairs) or even unpaired electrons can be achieved by standard topological analysis of well defined scalar functions. This procedure involves three steps: 1, evaluation of the ELF over a 3D grid; 2, localization of the critical points of the ELF, i.e., maxima, minima, and saddle points, defined by $\nabla \eta(r) = 0$; and 3, identification of the basin of each ELF maximum, i.e., all the points of the 3D grid from which if the $\nabla \eta$ is followed the trajectory terminates on the maximum considered.

Within this framework a partition of the molecular space into basins of maxima of the ELF having a clear chemical meaning can be achieved. These basins are either core basins located around the nuclei (for $Z > 2$) or valence basins in the remaining space. With this well defined mathematical partitioning of molecular space it is possible to integrate the electronic density

$\rho(r)$, over a given volume Ω_i , corresponding to basin i in order to calculate basin populations,

$$\langle N(\Omega_i) \rangle = \int_{\Omega_i} \rho(r) dr, \quad (6)$$

and the associated variance of the basin population given by

$$\sigma^2(\langle N \rangle, \Omega_i) = \langle N^2 \rangle_{\Omega_i} - \langle N \rangle_{\Omega_i}^2. \quad (7)$$

This quantity measures the variance of the quantum mechanical uncertainty of the basin population which may be interpreted in terms of electron delocalization. It may be written in terms of contributions arising from other basins according to

$$\sigma^2(\langle N \rangle, \Omega_i) = \sum_{j \neq i} \langle N \rangle_{\Omega_i} \langle N \rangle_{\Omega_j} - \langle N \rangle_{\Omega_i, \Omega_j}^2 = \sum_{j \neq i} B_{ij}. \quad (8)$$

In equation (8), $\langle N \rangle_{\Omega_i} \langle N \rangle_{\Omega_j}$ are the numbers of electron pairs classically expected from the basin population, whereas $\langle N \rangle_{\Omega_i, \Omega_j}^2$ is the actual number of pairs obtained by integration of the pair function over the basins Ω_i and Ω_j . The quantity B_{ij} is the covariance defined as $B_{ij} = \langle (N_i - \langle N \rangle_i)(N_j - \langle N \rangle_j) \rangle$. The pair covariance B_{ij} indicates how much the populations of two given basins are correlated.

The ELF calculations were performed with the TopMoD package [32, 37] and the isosurfaces have been visualized using SciAn software [38]. The TopMod program requires a wavefunction file generated by Gaussian98 [39]. With evaluation of the ELF grid file and identification of the different basins and associated attractors, TopMod calculates the electron population in the different molecular space partitions or basins.

The goal of the ELF analysis is to provide a clear picture of how the electron population, the making and breaking of bonds, and charge transfer are affected by the adsorption and dissociation of CO on our cluster surface representation of Cr(110). The ELF approach provides a better description of the electron distribution and associated properties than the Mulliken population analysis used in our earlier study [4].

4. Results and discussion

4.1. DMC computations

We used a trial function consisting of a product of a restricted HF function, and a Schmidt–Moskowitz correlation function [27] (equation (4)). In addition to Cr, SBK ECPs were also used for C and O. The reliability of these functions for first- and second-row atoms is well established [13, 39, 40].

As in our *ab initio* HF study, the Cr interatomic distance was set to the experimental bcc lattice constant of

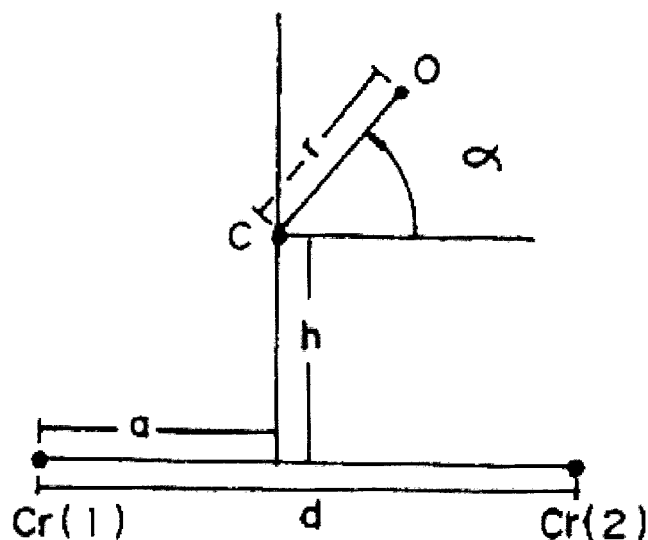


Figure 1. Geometries used for the near-parallel and the perpendicular orientations of CO on a dimer model surface of Cr(110).

the bulk nearest neighbour distance for Cr(110) of 2.498 Å (all bond distances are in Å). The distance between C and the surface is 1.935 Å for the perpendicular configuration from our earlier study, which compares favourably with the experimental CrC distance in Cr(CO)₆ of 1.92 Å, and the CO geometry was that optimized in [4], 1.149 Å, which is in agreement with experiment (1.15 Å). In the tilted orientation, we have used an optimized CO distance of 1.233 Å, the height of C above the CrCr bond as 1.581 Å, the inclination angle of CO to CrCr as 11.3° and the distance between the CO and CrCr bond axis as 1.366 Å from our previous study [4] (figure 1).

Trial wavefunction optimization was carried out using the recently developed absolute value functional for a fixed sample [41]. This optimization scheme is quite stable and does not show numerical instabilities during the minimization. Trial function optimization with imposed cusp conditions in this approach recovers more correlation energy than the widely used variance minimization procedure. With 60 iterations, parameter convergence is attained to 0.0001 for the Schmidt–Moskowitz correlation function. The absolute value functional technique significantly reduced local energy fluctuations after three optimizations (table 1).

Table 2 presents the total energies from DMC of the Cr₂CO molecule for the two geometries. As expected from our previous study, the tilted configuration is energetically favoured. This stable binding mode of molecular CO chemisorption on Cr(110) consists of CO adsorbed with the molecular axis approximately parallel or tilted to the surface, as was identified experimentally by Shinn and Madey using HREELS as the only CO binding mode at low coverage [9]. This is understandable from the present study, considering the 1.9 eV greater stability of the tilted configuration. Other experiments including Auger electron spectroscopy (AES) [9] confirm this finding; they demonstrate that the near-parallel orientation undergoes dissociation upon heating to $T > 200$ K and indicate that this mode serves as a precursor state to CO dissociation. ESDIAD studies for different metals such as Ru(001) support the model involving parallel adsorption of CO molecules by the metallic surface [10]. On this surface there is a large reduction in molecular binding for perpendicular adsorption relative to the bent near-parallel geometry for adsorption.

Table 1. Optimization using the absolute value functional (absolute deviation minimization in E_h).

Optimization	Tilted configuration		Perpendicular configuration	
	Initial	Final	Initial	Final
1st	6.742 624	2.555 961	6.200 884	2.492 217
2nd	2.254 479	2.184 730	2.327 177	2.247 538
3rd	2.228 339	2.226 472	2.246 985	2.242 024

Table 2. DMC energies (in eV) for Cr₂CO in the tilted/near-parallel and perpendicular configurations.

	Tilted configuration	Perpendicular configuration	Difference
DMC energy	-194.0569 (0.0020)	-193.9866 (0.0020)	0.0703 (0.0040)

It is worth noting that the large 1.9 eV energy difference between the two geometries agrees well with semi-empirical results based on the Hückel Hamiltonian [11]. The tilted/near-parallel configuration is a consequence of strong π and 5σ donation bonds whose antibonding counterparts are empty [1, 3]. The DMC energy difference is considerably larger than that obtained in our *ab initio* HF study [4].

4.2. ELF analysis

The results of the ELF topological study of the interaction of CO with the model surface are presented in figures 2–4. It has been shown that this topological description is structurally stable in the sense that the number and type of ELF partitioning plus their evolution are not dependent on the quantum mechanical method used in determining the ELF. For convenience, we have chosen the DFT/B3LYP method with with 6-31G** basis set for the present ELF analysis. To see clearly the effect of CO adsorption on the surface and how electron populations change, we have carried out a topological analysis with the two Cr atoms at the experimental separation for Cr(110) in the absence of CO.

Figure 2 shows the ELF molecular partitioning of the two isolated Cr atoms. We label here core basins C(Cr1) and

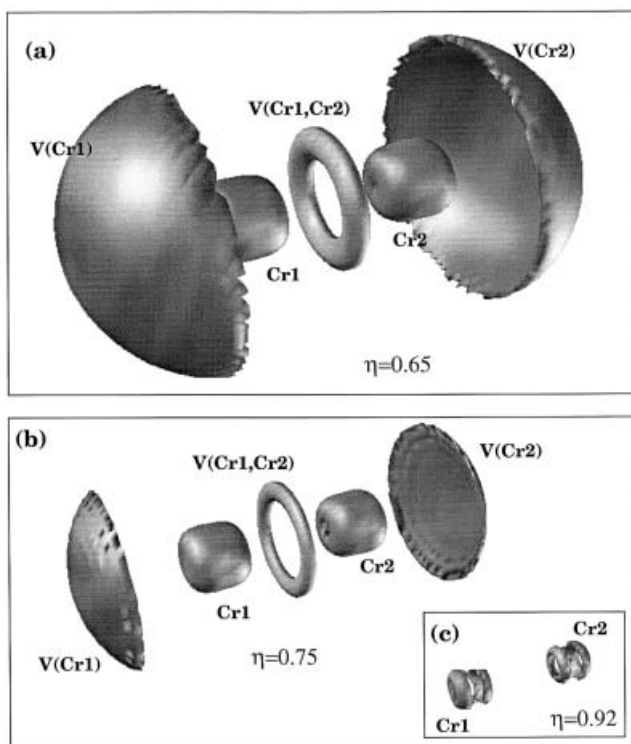


Figure 2. Electron localization function (ELF) analysis for the dimer model of the Cr(110) surface: (a) the ELF isosurface for $\eta = 0.65$; (b) the two Cr atoms for $\eta = 0.75$, and (c) the two Cr atoms for $\eta = 0.92$.

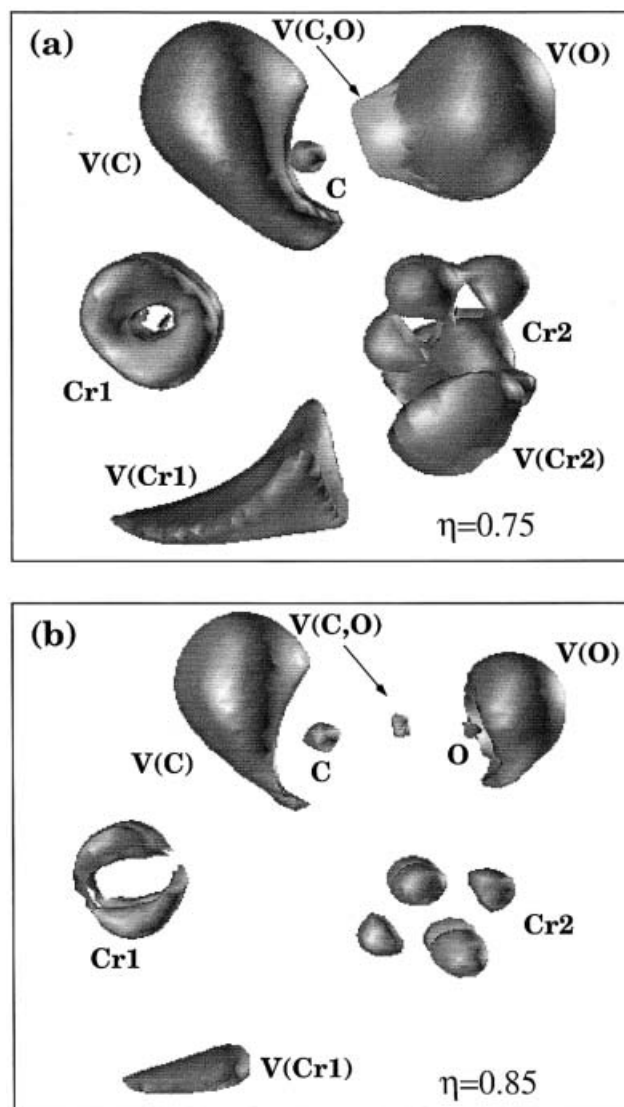


Figure 3. ELF representation of CO adsorption on the Cr(110) dimer model surface: parallel orientation of CO to Cr₂.

C(Cr2), two monosynaptic valence basins V(Cr1), V(Cr2), corresponding to lone pairs of electron, and disynaptic basin V(Cr1,Cr2), associated with the bonding of the two Cr atoms. If we examine the molecular space for large ELF values, we see that the different initially compact basins start to separate from each other. Figure 2 (a) displays the ELF isosurface for $\eta = 0.65$. Basin populations, are obtained from integration of the one-electron density $\rho(r)$ over these basins, are given in table 3. The population of the V(Cr1,Cr2) basin is 2.04 electrons, indicating a single covalent bond, whereas the torus shape of this basin is similar to the triple bond in acetylene [33]. The valence basins V(Cr1) and V(Cr2) have a population of 0.88 electrons. Accordingly, the total

Table 3. Basins, populations and standard deviation of the 2 Cr atoms.^a

Basin	Population	Standard deviation (σ)	η^b
C(Cr1)	22.10	2.60	0.99
C(Cr2)	22.10	2.60	0.99
V(Cr1)	0.88	0.58	0.78
V(Cr2)	0.88	0.58	0.78
C(Cr1,Cr2)	2.04	1.50	0.75

^aThe Cr atoms are separated by the lattice distance for Cr(110) of 2.498 Å.

^bELF value.

valence charge on each Cr atom is 1.90 electrons. The rest of the charge, 22.10 electrons, is contained within the two core basins indicated in figure 2 by Cr1 and Cr2 and coincide with the location of the nuclei. The shape along with the basin population of V(Cr1,Cr2) may be under-

stood by considering (i) the symmetry of the system ($D_{\infty h}$) and (ii) the effect of Pauli repulsion. Note that the stronger the Pauli repulsion, the lower the ELF values for V(Cr1,Cr2) (table 4) and the smaller the basin population. The torus shape of V(Cr1,Cr2) satisfies the above requirements. The classification of the CrCr bond is not straightforward because the low V(Cr1,Cr2) population and the large delocalization between the metallic cores is confirmed by a standard deviation of 2.60 electrons (table 3) of each Cr core indicated by Cr1 and Cr2 in figure 2.

The origin of the low value of the V(Cr1,Cr2) population, compared with that expected based on the 'nominal bond order' is certainly due to the character of the d atomic orbitals. They may be considered either as core orbitals or valence orbitals, depending on the chemical system under scrutiny. In the case of metallic solids, it has been found that the TM d orbitals contribute very

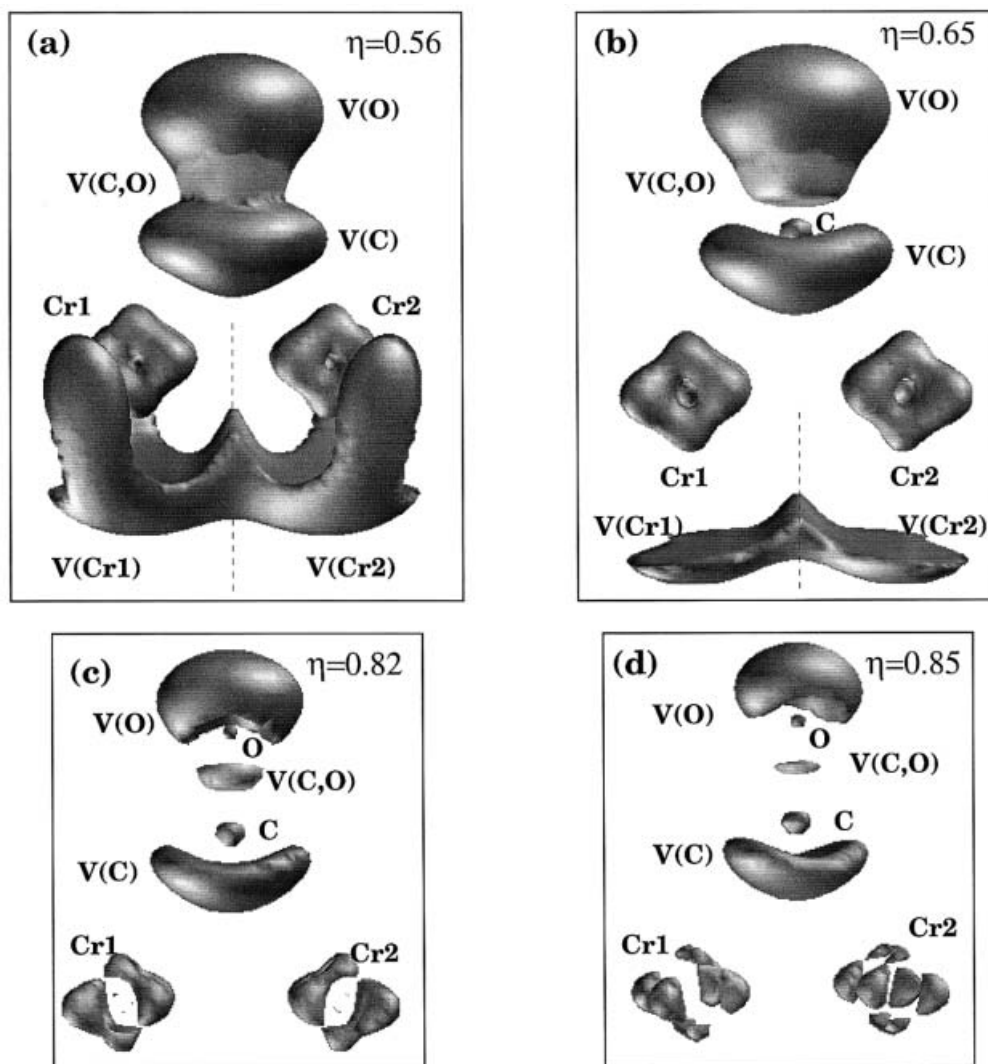


Figure 4. ELF representation of CO adsorption on the Cr(110) dimer model surface: perpendicular orientation of CO to Cr₂.

Table 4. Basins and orbital contributions of the six last occupied orbitals.

Basin	Orbital contributions					
	σ_g	π_u	π_u	δ_g	δ_g	σ_u
C(Cr1)	0.32	0.84	0.84	0.91	0.91	0.37
C(Cr2)	0.32	0.84	0.84	0.91	0.91	0.37
V(Cr1)	0.26	0.02	0.02	0.02	0.03	0.52
V(Cr2)	0.26	0.02	0.02	0.02	0.03	0.52
V(Cr1,Cr2)	0.82	0.29	0.29	0.13	0.13	0.19

little to the interstitial density [35]. Note that the experimental lattice bcc bulk distance (2.498 Å) separating Cr atoms on the Cr (110) surface is larger than the optimum distance between Cr atoms in the dimer (1.679 Å) and corresponds to a single bond between diffuse singly occupied 4s orbitals, while the d electrons remain localized on the cores. In the present case, the orbital contributions (table 4) to the core and V(Cr1,Cr2) populations provide the pertinent information: the molecular orbitals essentially contribute to the core populations.

The main characteristic of CrCr bonding is the covariance between the two Cr core basins. In general, the standard deviation between two core basins is about 0.1–0.5 electron; however, we have found a standard deviation of 2.60 electrons between the Cr cores. Such large fluctuations lead us to introduce a resonance structure between the Cr cores. In fact, the two Cr atoms are in a closed-shell singlet state. There is no spin polarization and each core is considered to be in a local closed-shell structure whose orbitals satisfy $D_{\infty h}$ point group symmetry conditions. The population of each Cr core is ~ 22 electrons and hence 4 electrons out of the 6 formally considered as valence from MO theory should now be considered as core electrons. Moreover, each Cr atom participates with one 4s electron in the V(Cr1,Cr2) population and has one electron in its valence basin, namely, V(Cr1) and V(Cr2). Accordingly, there are four electrons occupying molecular orbitals arising from d orbitals included in core basins. In a resonance description we assume that each of the Cr cores may adopt either of the configurations, Cr:[Ar] d^4 or Cr:[Ar] d^2 . Using these core configurations, we form the following resonance structures:



Both resonance descriptions 9(a,b) yield an average population of 22 electrons for the Cr core basins. The first has a standard deviation of zero electrons while the value for the second one is 4 electrons. The calculated standard deviation of 2.60 electrons can be recovered

Table 5. Basins, populations and standard deviation of the tilted/near-parallel configuration of CO inclined to the model Cr Surface.

Basin	Population	Standard deviation (σ)	η^a
C(Cr1)	22.71	1.54	0.99
C(Cr2)	22.43	1.25	0.99
C(O)	2.09	0.12	1.00
C(C)	2.09	0.23	1.00
V(O)	5.41	1.58	0.90
V(C)	3.85	1.42	0.96
V(Cr1)	0.90	0.59	0.90
V(Cr2)	0.62	0.30	0.78
V(C,O)	1.90	1.11	0.87

^aELF value.

approximately assuming that this first resonant structure contributes with a coefficient of $\sim 1/3$ and the second with a coefficient of $\sim 2/3$.

In conclusion the chromium d orbitals determine the metal–metal interactions through their involvement in the delocalization of the electronic density between the two cores and the V(Cr1,Cr2) bonding basin. This approach is an alternative to the description of the CrCr bond provided by MO theory. The total valence charge on each Cr atom is 1.90 electrons. The rest of the charge, 22.1 electrons, is contained within the two core basins indicated in figure 2 by Cr1 and Cr2. In figure 2(b) the two Cr atoms are shown for $\eta = 0.75$. The Cr1 and Cr2 core basins have a cylindrical shape, as expected from the linear symmetry of the system. These basins are composed of s, p and d orbitals, and the inset figure presents its structure.

Figure 3 depicts the molecular structure of the Cr_2CO complex with the CO molecule tilted towards the CrCr axis, and shows that there is no longer a bond between the two Cr atoms. Moreover, there is no bonding basin between CO and the two Cr atoms. Atom Cr1 appears with the same local structure as in the two-atom system. Atom Cr2 appears, however, polarized by the oxygen lone pairs indicated by V(O) and appears with a local coordination of 6, indicated by the 6 basins around the position of the nucleus (figure 3(b)). The standard deviation for the two Cr core basins decreases to 1.54 electrons for Cr1 and 1.25 electrons for Cr2 (table 5) while the covariance between the two basins is 0.21. The CO molecule has its regular form: V(C,O) bonding basin, V(C) and V(O) lone pairs. The valence basin V(O) contains 5.41 electrons, 1.41 electrons more than expected for oxygen lone pairs. The remainder of the charge distribution and the standard deviations over the basins are listed in table 5.

The total number of electrons on CO is 15.34. This indicates charge transfer from the Cr atoms towards CO of about 1.34 electrons and is due mainly to charge transfer from the V(Cr1,Cr2) basin towards the V(O) basin. The 2-Cr complex has 46.66 electrons. In particular, Cr1 carries a charge of +0.39 and Cr2 a charge of +0.95. This charge distribution induces a dipole moment of 1.848 D. From the above analysis we conclude that the interaction between CO and the model 2-Cr surface is purely ionic.

The other interaction mode for this system is CO oriented perpendicular to the surface. This chemisorption process has the structure given in figure 4. The isosurfaces in this figure correspond to η of 0.56, 0.65, 0.82 and 0.85, values that measure the degree of localization. Figure 4(a) shows clearly that the valence of CO follows from the separated valence of the two Cr atoms. The CO valence splits at a higher value of the ELF, as shown in figure 4(b). In this geometry both Cr1 and Cr2 have local coordination 6 (figure 4(d)). In figure 4(a, b) the dashed line shows the separation between the Cr1 and Cr2 valences, 0.90 electron for each atom (table 6). Each of the two ensembles of non-bonding Cr1 and Cr2 contains 22.50 electrons. Figure 4(b, c, d) shows the ELF function η for increasing values culminating in very localized CO and two Cr atoms. From table 6 we conclude that CO carries a total of 15.20 electrons or, alternatively, a net charge of -1.20 , and each of the Cr atoms carries a net charge of $+0.60$. This charge distribution induces a dipole moment of 0.5578 D. From this analysis we conclude that the interaction between CO and our model surface is strongly ionic. The Cr cores are split because of the polarization of d orbitals due to the environment. The tilted configuration considerably polarizes the second Cr atom because of the oxygen lone pairs. This behaviour disappears for the perpendicular configuration because the lone pair on carbon plays the role of a bonding basin.

Table 6. Basins, populations and standard deviation of the perpendicular configuration of CO to the model Cr surface.

Basin	Population	Standard deviation (σ)	η^a
C(Cr1)	22.50	1.73	0.99
C(Cr2)	22.50	1.73	0.99
C(O)	2.20	0.39	1.00
C(C)	2.20	0.26	1.00
V(O)	4.46	1.44	0.91
V(C)	3.60	1.66	0.94
V(Cr1)	0.90	0.76	0.75
V(Cr2)	0.90	0.76	0.75
V(C,O)	2.74	1.76	0.87

^a ELF value.

Typically the transfer of charges is larger when CO is tilted (near-parallel configuration). The Cr₂CO interaction model shows general features of charge transfer from the 5 σ orbital of CO to unoccupied Cr orbitals, followed by back donation of d electrons from the Cr surface to unoccupied 2 π^* CO orbitals, which are important in explaining the dissociation of CO.

5. Conclusion

We have carried out DMC calculations for the ground state energy of a Cr₂CO model for the interaction of CO with the Cr(100) surface. This system yields useful insight into the adsorption of CO on Cr metal surface and may hold value for other 3d metal surfaces. The present results are consistent with various experiments that show the tilted/near-parallel configuration to be a more stable orientation mode for low CO coverage than the perpendicular arrangement. We have determined the energy difference between these two modes of CO-surface interaction to high accuracy. The adsorption of CO on the model surface have been analysed in terms of the topological representation of the electron localization function (ELF). This procedure provides a clear understanding of the electron rearrangement and reorganization during the interaction of CO with the metallic surface. The CO dissociation on 3d metal surfaces is confirmed to be a two-step (metal \rightarrow CO and CO \rightarrow metal) charge transfer process, and the near-parallel orientation (tilted state) is identified as the precursor state to the dissociation.

O.E.A. and W.A.L. were supported by the Director, Office of Science, Office of Basic Energy Sciences, Chemical Sciences Division of the US Department of Energy under Contract No. DE-AC03-76SF00098. C.A.T., T.C.G. and A.C.P. acknowledge financial assistance from CNPq (Brazil). The calculations were carried out at the National Energy Research Supercomputer Center (NERSC).

References

- [1] TAFT, C. A., GUIMARAES, T. C., PAVAO, A. C., and LESTER JR., W. A., 1999, *Intl Rev. phys. Chem.*, **18**, 163.
- [2] PAVAO, A. C., TAFT, C. A., GUIMARAES, T. C. F., LEO, M. B. C., MOHALLEM, J. R., and LESTER JR., W. A., 2001, *J. phys. Chem. A*, **105**, 5.
- [3] PAVAO, A. C., GUIMARAES, T. C., LIE, S. B., TAFT, C. A., and LESTER JR., W. A., 1999, *J. molec Struct. Theochem*, **458**, 99.
- [4] PAVAO, A. C., HAMMOND, B. L., SOTO, M. M., LESTER JR., W. A., and TAFT, C. A., 1995, *Surface Sci.*, **323**, 340.
- [5] CEYER, S. T., 1988, *Ann. Rev. phys. Chem.*, **39**, 479.
- [6] GUIMARAES, T. C., PAVAO, A. C., TAFT, C. A., and LESTER JR., W. A., 1997, *Phys. Rev. B*, **56**, 7001; PAVAO,

- A. C., BRAGA, M., TAFT, C. A., HAMMOND, B. L., and LESTER JR., W. A., 1991, *Phys. Rev. B*, **44**, 1910.
- [7] BLYHOLDER, G., 1964, *J. chem. Phys.*, **68**, 2772; SUNG, S. S., and HOFFMANN, R., 1985, *J. Amer. chem. Soc.*, **107**, 578.
- [8] PAVAO, A. C., SOTO, M. M., LESTER JR., W. A., LIE, S. K., HAMMOND, B. L., and TAFT, C. A., 1994, *Phys. Rev. B*, **50**, 1868.
- [9] SHINN, N. D., and MADEY, T. E., 1985, *J. chem. Phys.*, **83**, 5928; 1984, *Phys. Rev. Lett.*, **53**, 2481.
- [10] PLUMMER, E. W., CHEM, C. T., FORD, W. K., EBERHARDT, W., MESSMERAND, R. P., and FREUND, H. J., 1985, *Surface Sci.*, **158**, 58.
- [11] MEHANDRU, S. P., and ANDERSON, A. B., 1986, *Surface Sci.*, **169**, L281.
- [12] BAGUS, P. S., NELIN, C. J., and BAUSCHLICHER, C. W., 1983, *J. chem. Phys.*, **28**, 5423; BAUSCHLICHER, C. W., BAGUS, P. S., NELIN, C. J., and ROOS, B. O., 1986, *J. chem. Phys.*, **85**, 354.
- [13] HARKLESS, J. A., and LESTER JR., W. A., 2001, *J. chem. Phys.*, **113**, 2680.
- [14] GROSSMAN, J. C., ROHLFING, M., MITAS, L., LOUIE, S. G., and COHEN, M. L., 2001, *Phys. Rev. Lett.*, **85**, 472.
- [15] PORTER, A. P., AL-MUSHADANI, O. K., TOWLER, M. D., and NEEDS, R. J., 2001, *J. chem. Phys.*, **114**, 7795.
- [16] GROSSMAN, J. C., LESTER JR., W. A., and LOUIE, S. G., 2000, *J. Amer. chem. Soc.*, **122**, 705.
- [17] CHRISTIANSEN, P. A., 1991, *J. chem. Phys.*, **95**, 361.
- [18] MITAS, L., and SHIRLEY, E. L., 1991, *J. chem. Phys.*, **95**, 3467; MITAS, L., 1994, *Phys. Rev. A*, **49**, 4411.
- [19] BELOHOREC, P., and ROTHSTEIN, S. M., 1993, *J. chem. Phys.*, **98**, 6401; ROTHSTEIN, S. M., 1996, *Intl J. Quantum Chem.*, **60**, 803.
- [20] FLAD, H.-J., and DOLG, M., 1997, *J. chem. Phys.*, **107**, 7951; SCHAUTZ, F., FLAD, H.-J., and DOLG, M., 1998, *Theoret. Chem. Accounts*, **99**, 231.
- [21] SOKOLOVA, S., and LUCHOW, A., 2000, *Phys. Rev. Lett.*, **320**, 421.
- [22] XIAO, C., HAGELBERG, F., OVCHARENKO, I. V., and LESTER JR., W. A., 2001, *J. molec. Struct. Theochem*, **549**, 181.
- [23] BARTLETT, R. J., WATTS, J. D., KUCHARSKI, S. A., and NOGA, J., 1990, *Chem. Phys. Lett.*, **165**, 513.
- [24] LESTER JR., W. S., 1997, *Recent Advances in Quantum Monte Carlo Methods* (Singapore: World Scientific); HAMMOND, B. L., LESTER JR., W. A., and REYNOLDS, P. J., 1994, *Monte Carlo Methods in Ab Initio Quantum Chemistry* (Singapore: World Scientific).
- [25] LUECHOW, A., and ANDERSON, J. B., 2000, *Ann. Rev. phys. Chem.*, **51**, 501; ANDERSON, J. B., 1999, *Rev. comput. Chem.*, **13**, 133.
- [26] FOULKES, W. M. C., MITAS, L., NEEDS, R. J., and RAJAGOPAL, G., 2001, *Rev. mod. Phys.*, **73**, 33; MITAS, L., and CEPERLEY, D. M., 1996, *Adv. chem. Phys.*, **93**, 1.
- [27] SCHMIDT, K. E., and MOSKOWITZ, J. W., 1990, *J. chem. Phys.*, **93**, 4172.
- [28] BOYS, S. F., and HANDY, N. C., 1969, *Proc. R. Soc. Lond. A*, **310**, 43.
- [29] STEVENS, W. J., BASCH, H., and KRAUSS, M., 1984, *J. chem. Phys.*, **81**, 6026.
- [30] KROKIDIS, X., SILVI, B., DEZARNAUD-DANDINE, C., and SAVIN, A., 1998, *New J. Chem.*, 1341; NOURY, S., KROKIDIS, X., FUSTER, F., and SILVI, B., 1999, *Comput. Chem.*, **23**, 597.
- [31] SELVI, B., and SAVIN, A., 1994, *Nature*, **371**, 683.
- [32] BADER, R. F. W., 1990, *Atoms in Molecules: A Quantum Theory* (Oxford University Press).
- [33] KROKIDIS, X., MORIARTY, N. W., LESTER JR., W. A., and FRENKLACH, M., 1999, *Chem. Phys. Lett.*, **314**, 534.
- [34] SILVI, B., and GATTI, C., 2000, *J. phys. Chem. A*, **104**, 947.
- [35] KROKIDIS, X., NOURY, S., and SILVI, B., 1997, *J. phys. Chem. A*, **101**, 7277.
- [36] BECKE, A. D., and EDGEcombe, K. E., 1990, *J. chem. Phys.*, **92**, 5397.
- [37] NOURY, S., KROKIDIS, X., FUSTER, F., and SILVI, B., 1997, Topological Molecular Description (TopMoD) Package (Paris: Universite Pierre et Marie Curie) available at http://www.lct.jussieu.fr/silvi/topmod_english.html
- [38] PEPKE, E., MURRAY, J., LYONS, J., and HWU, T.-Z., 1993, SciAn (Tallahassee, FL: Supercomputer Computations Research Institute, Florida State University).
- [39] GREEFF, C. W., and LESTER JR., W. A., 1997, *J. chem. Phys.*, **106**, 6412.
- [40] OVCHARENKO, I. V., LESTER JR., W. A., XIAO, C., and HAGELBERG, F., 2001, *J. chem. Phys.*, **114**, 9028.
- [41] ASPURU-GUZIK, A., COURONNE, O., OVCHARENKO, I., and LESTER JR., W. A., unpublished.